FEBS Letters 588 (2014) 3445–3453

journal homepage: www.FEBSLetters.org

Mode of membrane insertion of individual transmembrane segments in Mdl1 and Mdl2, multi-spanning mitochondrial ABC transporters

Kwangjin Park, Sung-jun Jung, Hyeonseong Kim, Hyun Kim *

School of Biological Sciences, Seoul National University, Seoul 151-747, South Korea

ARTICLE INFO

Article history:
Received 12 June 2014
Revised 25 July 2014
Accepted 3 August 2014
Available online 13 August 2014

Edited by A. Chattopadhyay

Keywords:
Mitochondria
Stop-transfer
Conservative sorting
Import
TIM23
Mgm1

ABSTRACT

The sorting of an individual transmembrane (TM) segment of multi-spanning membrane proteins by the TIM23 complex in the mitochondrial inner membrane is poorly understood. Using the Mgm1 fusion approach, we attempted to assess the membrane insertion of individual TM segments of Mdl1p and Mdl2p, mitochondrial ABC transporters. Although these transporters share high sequence similarity, our results show that their membrane sorting patterns differ and that specific residues in TM domains strongly influence membrane insertion or translocation. These data imply that TIM23-mediated membrane insertion highly depends on the TM domain sequence context.

1. Introduction

Approximately 1000 mitochondrial proteins are present in *Saccharomyces cerevisiae*, and the majority of these proteins are encoded in the nucleus [1]. They are synthesized as precursors by cytosolic ribosomes and are imported into one of the mitochondrial subcompartments: the outer membrane (OM), the intermembrane space (IMS), the inner membrane (IM) or the matrix.

Proteins destined for the inner membrane of the mitochondria pass through the outer membrane using the translocase of the outer mitochondrial membrane (TOM) complex. Proteins containing a hydrophobic sorting signal within the transmembrane (TM) domain following the cleavable matrix targeting sequence (MTS, or presequence) are inserted into the inner membrane by the TIM23 complex via the stop-transfer pathway [2-4]. In comparison, some of the inner membrane proteins are imported to the matrix by the TIM23 complex with the aid of the presequence translocase-associated motor (PAM) complex and are subsequently inserted from the matrix by Oxa1p [5,6], Mba1p [7] or Bcs1p [8]. This sorting mode is called the conservative sorting pathway [9-12]. Metabolite carrier proteins lacking an MTS are guided by small TIM proteins (Tim9p and Tim10p) to the TIM22 complex, which facilitates insertion into the inner membrane; this process is known as the carrier pathway [13-15].

Although many multi-spanning membrane proteins are present in the mitochondrial inner membrane, the membrane insertion mechanism of these proteins is not well understood, partly due to a lack of robust experimental techniques. *In vitro* mitochondrial import and protease protection assays have been usually used to define the topology and sorting pathways of inner membrane proteins. However, not every inner membrane protein is importable into the mitochondria in a cell-free system, and recombinant proteases are sometimes unable to access proteins that are already folded or assembled into a protein complex [8,16,17]. Previously, we demonstrated that an Mgm1 fusion protein (MFP) assay can be used as an alternative approach to characterize the sorting pathways of mitochondrial inner membrane proteins [18].

In this report, we tested the applicability of the MFP approach in determining membrane insertion modes for individual TM segments of multi-spanning membrane proteins using Mdl1p, the sorting pathway of which has been previously determined [19]. Next, we determined the insertion mode of the distinct TM domains of Mdl2p, whose sorting mechanism is unknown. Mdl2p exhibits 47% sequence identity to Mdl1p [20,21] and contains a putative MTS and six TM segments, similar to Mdl1p [22]. Despite high sequence similarities and sequence context, our data show that the individual TM segments of Mdl1p and Mdl2p have

* Corresponding author. Address: School of Biological Sciences, Building 504-421, Seoul National University, 1 Gwanak-ro, Gwanak-gu, Seoul 151-747, South Korea. Fax: +82 2 872 1993.
E-mail address: joy@snu.ac.kr (H. Kim).

http://dx.doi.org/10.1016/j.febslet.2014.08.001

significantly different membrane insertion modes. Particularly, TM3 of Mdl2p is inserted by the stop-transfer mode, whereas that of Mdl1p is not inserted via this process. Furthermore, critical residues in respective TM3 segments of Mdl1p and Mdl2p that dictate membrane insertion or import are identified in this study. The results suggest that the insertion of TIM23-mediated membrane insertion is highly dependent on the TM domain sequence context.

2. Materials and methods

2.1. Construction of plasmids

Each gene was amplified by PCR using the designed primer sets described previously [18]. Additionally, an overlap PCR [23] method was used to replace the TM5 of Mdl1p or Mdl2p with another natural TM domain (Sco2p, She9p, or Mba1p). All plasmids were prepared by yeast homologous recombination as previously described and confirmed by DNA sequencing [24,25].

2.2. Western blot analysis

Yeast transformants of W303-1a (*MATa*, *ade2*, *can1*, *his3*, *leu2*, *trp1*, *ura3*), W303-1a *rho*$^{-}$ [26], Δ*yta10* (*MATa*, *ade2–1*, *his3–11,15*, *yta10::HIS3MX6*, *trp1–1*, *leu2,112*, *ura3–52*) [27], the temperature-sensitive *pam16-3* mutant or the isogenic wild-type *PAM16* strain [28] carrying each plasmid were grown overnight in 5 ml of -Leu medium at 30 °C. The preparation of whole-cell lysates by trichloroacetic acid (TCA) precipitation, SDS–PAGE and Western blotting were followed as described in [18].

2.3. [S^{35}]-Met pulse-labeling and chase experiment

Plasmids encoding various Mdl2-MFPs, Mdl1 (1-3TM), or Mgm1p were transformed into the Δ*yta10* strain, the *pam16-3* mutant or its isogenic wild-type strain. In Fig. 3E, yeast transformants were grown at 24 °C in -Leu medium up to A_{600} 0.8–1, and three A_{600} units of cells were radiolabeled with 90 μCi (A_{600} unit of cells/30 μCi) of [S^{35}]-Met for 5 min at 30 °C. A total of 60 μl of 200 mM Met was added and incubated for various time points at the same temperature. In Fig. 4B, 1.5 A_{600} units of cells were radiolabeled with 50 μCi of [S^{35}]-Met per time point for 5 min at 30 °C. A total of 200 μl of 200 mM Met was added and incubated for the indicated time points at 30 °C. The samples were analyzed by SDS–PAGE and autoradiography as described in [18]. Protein bands were detected using a Fujifilm BAS-2500 system.

3. Results

3.1. Experimental set-up

We previously developed the MFP assay for determining the sorting pathway of mitochondrial inner membrane proteins [18]. This method utilizes a rhomboid cleavage region (RCR) of a dynamin-like mitochondrial fusion protein, Mgm1p, as a reporter for the import of the upstream segment into the matrix or for the insertion into the inner membrane [25]. A protein of interest is fused with the C-terminal domain of Mgm1p containing the RCR. If the fused protein is imported into the matrix, the RCR of Mgm1p enters the inner membrane and is cleaved by Pcp1p; subsequently, C-terminal Mgm1p (*s*-Mgm1p) is produced (Fig. 1A, i). However, if the fused protein is inserted into the inner membrane by the stop-transfer mechanism, a long Mgm1 fusion protein (L-MFP) is produced (Fig. 1A, ii). Alternatively, the formation of *s*-Mgm1p can occur for membrane proteins with two TM segments in which the first TM segment is laterally inserted into the membrane and the second TM segment is inserted by the downstream C-terminal flanking loop being pulled into the matrix, as observed in Cyt1p and Yta10p (Fig. 1A, iii) [18,29]. However, if the two TM domains insert as a hairpin with an N_{matrix}–C_{matrix} orientation (Fig. 1A, iv), *s*-Mgm1p can also be formed. Thus, a limitation of the MFP approach is the inability to distinguish forms i and iv in Fig. 1A.

Despite this limitation, the ability of the MFP assay to distinguish between the former three possibilities may provide valuable information about the mode of membrane insertion for individual TM segments in multi-spanning inner membrane proteins. To test the efficacy of the MFP assay for this purpose, we chose the inner membrane protein Mdl1p as a model; the insertion mechanism of Mdl1p has been studied by *in vitro* import and proteinase K protection assays [19]. Mdl1p is a half-size inner-membrane mitochondrial ABC transporter that functions in the export of cleaved peptides derived from the *m*-AAA dependent mitochondrial quality control system [30]. Md11p has an MTS (1–59 residues [31]) and six TM domains (Table 1). We sequentially truncated the protein after each TM segment and fused each version with the C-terminal domain of Mgm1p containing the RCR (Fig. 1B). Three copies of hemagglutinin epitope tags (HA) were fused to the C-terminal end of Mgm1p for detection by Western blotting.

3.2. TM1–2 of Mdl1p is inserted into the inner membrane from the IMS

A previous report by Bohnert et al. showed that the first two N-terminal TM segments (TM1–2) are inserted by the stop-transfer mechanism, whereas the middle two TM segments (TM3–4) are sorted by Oxa1-mediated conservative sorting. The insertion of the last two TM segments (TM5–6) was not dependent on Oxa1; as a result, it was concluded that TM5–6 may be sorted by the stop-transfer mechanism [19].

Sequentially truncated Mdl1-MFP constructs were expressed in a wild-type (WT) yeast strain. Whole cell lysates from each yeast transformant were analyzed by SDS–PAGE and Western blotting. The major product of Mdl1 (1TM) was L-MFP, indicating that the TM1 is sorted by the stop-transfer mechanism (Fig. 2A). The remainder of the fusion constructs, Mdl1(1–2TM), Mdl1(1–3TM), Mdl1(1–4TM), Mdl1(1–5TM), and Mdl1(1–6TM), produced *s*-Mgm1p as a major product (Fig. 2A). The *m*-AAA complex can dislocate TM segments [27,32]. Thus, to determine whether the formation of *s*-Mgm1p resulted from the dislocation activity of the *m*-AAA complex or from matrix import by the TIM23 complex, a set of Mdl1-MFP constructs were expressed in an *m*-AAA defective (Δ*yta10*) strain (Fig. 2A). Mdl1(1–2TM) expressed in the Δ*yta10* strain showed increased L-MFP compared to WT, but for the remainder of the constructs, there was essentially no difference in the formation of L-MFP and *s*-Mgm1p between the constructs expressed in the WT and Δ*yta10* strains, demonstrating that L-MFP and *s*-Mgm1p were formed by the TIM23 complex. Because TM1 is inserted into the inner membrane by the stop-transfer mode, the formation of *s*-Mgm1p in Mdl1(1–2TM) indicates that TM2 is sorted by a loop insertion, as observed for the inner membrane proteins Cyt1p and Yta10p [18,29] (Fig. 2B). None of fusion constructs carrying TM3 generated L-MFP. These results suggest that TM3–6 are not sorted by the stop-transfer mode. As mentioned above, the MFP approach cannot distinguish whether TM3–4/TM5–6 are inserted as hairpins with an N_{matrix}–C_{matrix} orientation or whether TM3–4/TM5–6 are imported into the matrix (Fig. 2B). However, because Bohnert et al. previously demonstrated that TM3–4 membrane insertion is dependent on Oxa1 and is thus processed by the conservative sorting pathway [19], TM3–4 are most likely imported into the matrix by the TIM23 complex.

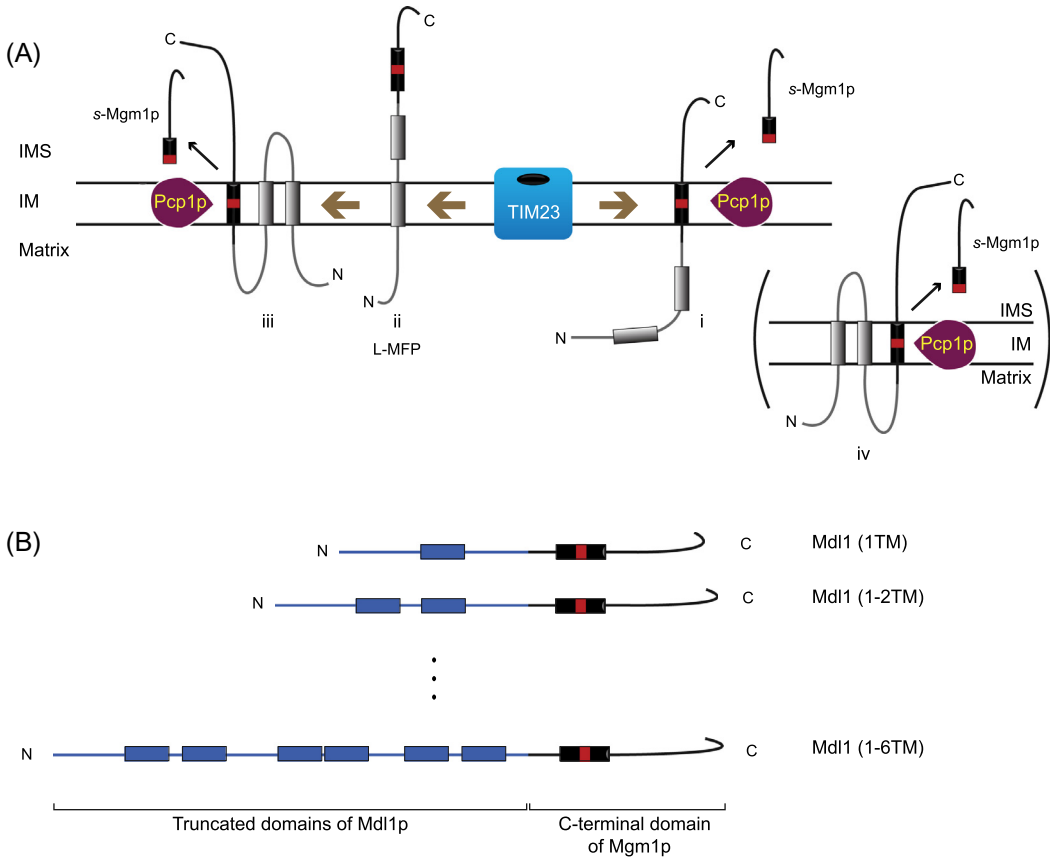

Fig. 1. Schematic representation of the Mgml fusion approach. (A) Formation of the long Mgm1 fusion protein (L-MFP) and short Mgm1p isoform (*s*-Mgm1p) are illustrated. (B) Mdl1p (blue), which contains six TM segments, was sequentially truncated and fused to the Mgm1p reporter domain (black). The number of the TM segments (blue box) of Mdl1p is in parentheses. The Rhomboid cleavage region (RCR) (red) is present in the TM segment (black box) of the C-terminal domain of Mgm1p. IMS, intermembrane space; IM, inner membrane; Pcp1p, rhomboid intramembrane protease.

Table 1
Information for TM domains of Mdl1p and Mdl2p.

Name (systematic name)	TM	Predicted TM sequence	ΔG_{app} (kcal/mol)
Mdl1p (YLR188w)	1	^{102}YIGLALLLILISSSVSMAVPS^{122}	0.66
	2	^{157}TALGAVFIIGAVANASRIIIL^{177}	0.6
	3	^{233}DGTRAIIQGFVGFGMMSFLSW^{253}	2.37
	4	^{255}LTCVMMILAPPLGAMALIYGR^{275}	0.8
	5	^{337}GLFFGSTGLVGNTAMLSLLLV^{357}	1.5
	6	^{373}SSFMMYAVYTGSSLFGLSSFY^{393}	3.5
Mdl2p (YPL270w)	1	^{115}DWKLLLTAILLLTISCSIGMS^{135}	-0.4
	2	^{172}SFFTVALLIGCAANFGRFILL^{192}	-0.28
	3	^{248}DGVKALICGVVGVGMMCSLSP^{268}	2.1
	4	^{270}LSILLLFFTPPVLFSASVFGK^{290}	1.39
	5	^{352}AKFFTTTSLLGDLSFLTVLAY^{372}	1.9
	6	^{388}TAFMLYTEYTGNAVFGLSTFY^{408}	4.2
Sco2p (YBR024w)	1	^{79}RWKATIALLLLSGGTYAYL^{97}	0.08
She9p (YDR393w)	1	^{296}TWGTFILMGMNIFLFIVLQLLL^{317}	-1.98
Mba1p (YBR185c)	1	^{74}VFAHPLIVANALIRRLYTF^{92}	2.32

The TM domains are predicted by TOPCONS [39], and the free energy of membrane insertion for each TM segment is calculated by the ΔG predictor [40].

3.3. TM5 of Mdl1p is translocated into the matrix

A previous work in [19] suggested that TM5 may be membrane-inserted by the stop-transfer mechanism, thus we wanted to determine the membrane insertion of TM5 of Mdl1 in more detail. We prepared additional MFP constructs in which the TM5 of Mdl1p was replaced with a TM segment processed by known sorting pathways (Fig. 2C). TM segments of Sco2p and She9p are sorted by the stop-transfer mechanism, whereas the TM segment of Mba1p is sorted by the conservative sorting mechanism [7,9,33,34]. When these fusion constructs were expressed in the WT yeast strain, only *s*-Mgm1p was detected (Fig. 2D, left panel). It was considered, however, that the replacement of the TM domain of Mdl1p caused the *m*-AAA protease to recognize the foreign TM domain and dislocate it from the inner membrane. Thus, we expressed the fusion proteins in the *m*-AAA-defective strain (Δ*yta10*), and protein samples were analyzed (Fig. 2D, middle panel). When TM5 from Mdl1p was replaced by the TM segment from Sco2p or She9p, the major product was L-MFP for the 1–5TM constructs in the Δ*yta10* strain, indicating that the altered

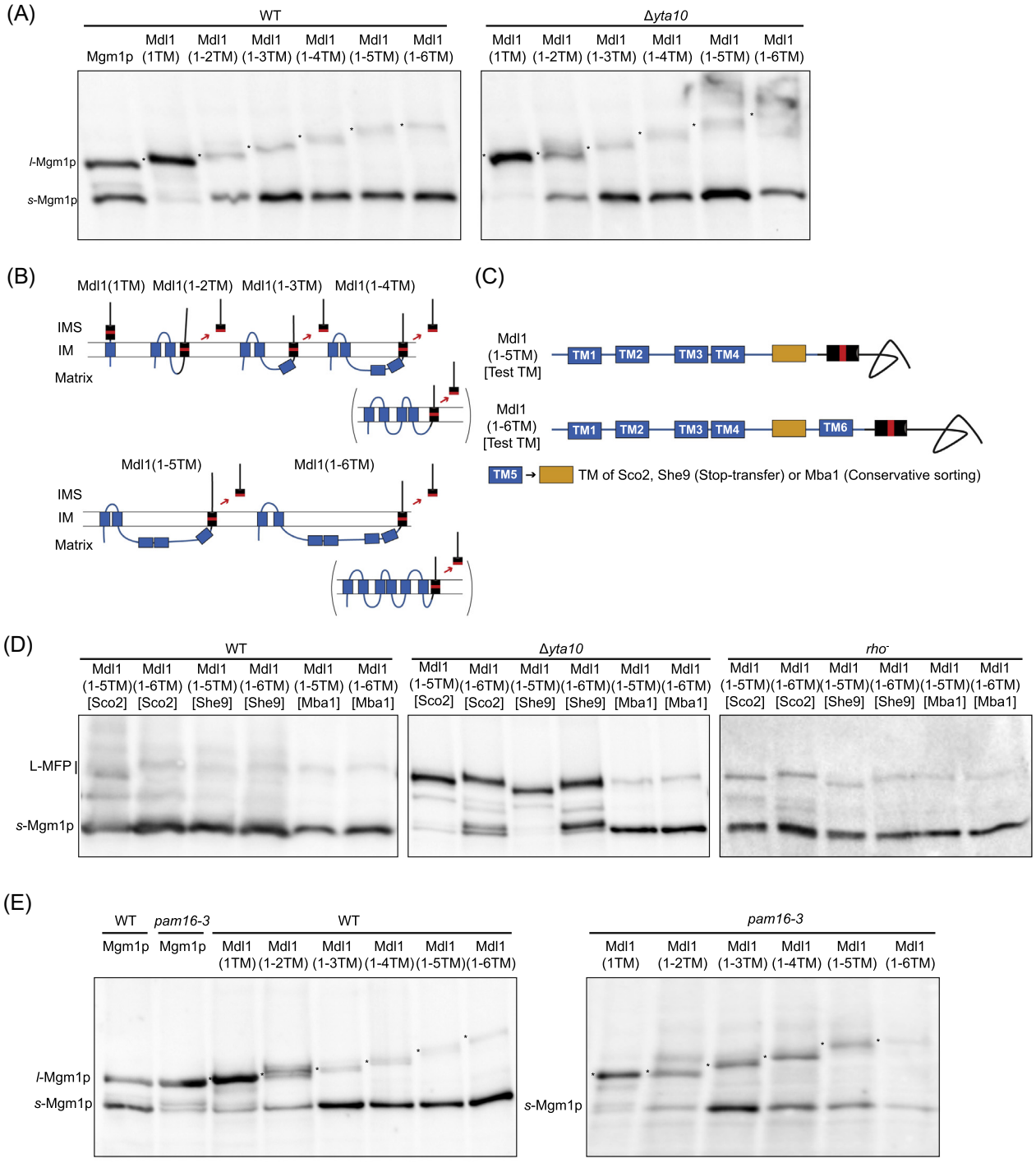

Fig. 2. Membrane insertion modes for individual TM segments of Mdl1p. (A) Mgm1p and the indicated Mdl1-MFPs were expressed in W303-1a and Δ*yta10* yeast strains. The number of TM segments fused to the C-terminal domain of Mgm1p is noted in parentheses. (B) Schematic representation of membrane insertion or the import of TM domains of Mdl1-MFPs. (C) TM5 segments (blue box) from Mdl1(1–5TM) and Mdl1(1–6TM) were exchanged with the natural TM (orange box) from two stop-transfer sorted proteins (Sco2p, She9p) or a conservative-sorted protein (Mba1p). Mdl1-MFP constructs were expressed in W303-1a, Δ*yta10*, and W303-1a *rho*$^{-}$ strains (D) and the *pam16-3* mutant or its isogenic WT strain (E). Cells were grown at 30 °C, whole cell lysates were subjected to SDS–PAGE and Western blot analysis with an anti-HA antibody. The *l*- and *s*-Mgm1p are shown on an SDS-gel as a reference. L-MFP is indicated with *asterisks*. *l*-Mgm1p, long Mgm1 isoform; *s*-Mgm1p, short soluble Mgm1 isoform; L-MFP, long Mgm1 fusion protein.

TM segment was membrane inserted by the TIM23 complex but dislocated by the *m*-AAA protease (Fig. 2D). Therefore, the levels of L-MFP and *s*-Mgm1p produced in the Δ*yta10* strain represent the forms produced by the TIM23 complex, whereas L-MFP and *s*-Mgm1p observed in the WT strain can be attributed to the actions of either the TIM23 complex or the *m*-AAA protease. Thus, we consistently assessed formation of L-MFP and *s*-Mgm1p in both WT and Δ*yta10* strains. Yta10 deletion cells are respiratory-deficient due to the impaired assembly of respiratory chain complexes. Hence, to establish whether the formation of L-MFP and *s*-Mgm1p in the Δ*yta10* strain results from general respiratory defects as opposed to the impaired dislocation activity of *m*-AAA,

we expressed the constructs in a respiratory-deficient W303-1a *rho*$^-$ strain [26], which carries truncations in the mitochondrial genome (Fig. 2D, right panel). Although little more L-MFP forms for the Sco2 and She9 constructs were observed in the *rho*$^-$ strain compared to the WT strain (Fig. 2D, left and right panels), significantly less amounts of L-MFP forms were detected in the *rho*$^-$ strain for the Sco2 and She9 constructs (Fig. 2D, middle and right panels). Therefore, these results suggest that the majority of L-MFP formed in the Δ*yta10* strain result from impaired dislocation activity of the *m-AAA* complex rather than general defects of mitochondria. Interestingly, while Mdl1(1–5TM)[Sco2]/[She9] constructs generated only L-MFP, the presence of the downstream segment in Mdl1(1–6TM)[Sco2]/[She9] led to the increased formation of *s*-Mgm1p. These results suggest two possibilities: (1) the presence of an upstream strong stop-transfer segment facilitated the insertion of TM6 from the IMS or (2) the presence of a downstream TM segment caused the import of both TM5 and TM6 into the matrix. The strong stop-transfer signal on TM5 suggests that the former possibility is more likely. Mdl1(1–5TM)[Mba1] and Mdl1(1–6TM)[Mba1] mainly produced *s*-Mgm1p, similar to Mdl1(1–5TM) and Mdl1(1–6TM) in both the WT and Δ*yta10* strains, indicating that the TM domain of Mba1p was translocated into the matrix by the TIM23 complex (Fig. 2D). Based on insertion patterns of these control MFPs, we conclude that TM5 of Mdl1p is not sorted by the stop-transfer mechanism.

3.4. The PAM complex mediates the import of TM3–6 of Mdl1p

The PAM complex, consisting of Pam16p, Pam17p, Pam18p, mtHsp70, Mge1p and Tim44p, modulates the translocation of proteins into the matrix [4,28,35,36]. Therefore, impaired PAM machinery function leads to defects in the import of matrix-targeted proteins [28]. In case of Mgm1p, defective PAM function impairs the import of Mgm1p; therefore, the formation of the *s*-Mgm1p isoform was reduced [37] (Fig. 2E). A previous study showed that the import of TM3–6 of Mdl1p was impaired in a strain defective in mtHsp70 function [19]. To assess the effects of the PAM complex in the translocation and membrane insertion of Mdl1-MFPs, we expressed these proteins in a temperature-sensitive import motor defective (*pam16-3*) strain and its isogenic wild-type strain. The relative amounts of *s*-Mgm1p from Mdl1(1–3TM), Mdl1(1–4TM), Mdl1(1–5TM), or Mdl1(1–6TM) were decreased in the *pam16* mutant strain compared to the WT strain, suggesting that a functional PAM complex is required for the efficient import of TM3–6 of Mdl1p.

3.5. Membrane insertion of Mdl2p

Next, we determined the membrane insertion of the MTS-containing mitochondrial multi-spanning membrane protein Mdl2p, a homolog of Mdl1p. Mdl2p contains six predicted TM domains, and the hydrophobicity of the Mdl2p TM domains is similar to that of the Mdl1p TM domains (Table 1). As performed with Mdl1p, Mdl2p was systematically truncated after each TM domain and fused with the C-terminal domain of Mgm1p. Mdl2-MFP constructs were expressed in WT and Δ*yta10* yeast strains, and whole cell lysates were analyzed (Fig. 3A). For Mdl2 (1TM) and Mdl2 (1–3TM), L-MFP was the major product, suggesting that TM1 and TM3 are sorted by the stop-transfer mechanism. The other constructs, Mdl2 (1–2TM), Mdl2 (1–4TM), Mdl2 (1–5TM) and Mdl2 (1–6TM), produced mainly *s*-Mgm1p (Fig. 3A). Given that TM1 and TM3 are laterally inserted into the inner membrane, TM2 must be inserted as a loop from the IMS (Fig. 3B). For TM4, because the size of the loop between TM3 and TM4 is only one residue, it is highly likely that TM4 is inserted from the IMS into the inner membrane (Fig. 3B). Furthermore, these results suggest that Mdl2 TM5 is not inserted by the stop-transfer mechanism in the absence of TM6, but as explained earlier in the presence of TM6, we cannot distinguish between the two possibilities of TM5–6 hairpin insertion and TM5–6 import (Fig. 3B).

To determine the insertion mechanism of TM5 in more detail, TM5 was replaced with a TM segment of Sco2p (stop-transfer), She9p (stop-transfer) or Mba1p (conservative sorting) in Mdl2 (1–5TM) and Mdl2 (1–6TM), as performed for Mdl1p. These constructs were expressed in WT and Δ*yta10* yeast strains (Fig. 3C). While Mdl2(1–5TM)[Sco2 or She9] and Mdl2(1–6TM)[Sco2 or She9] produced mostly L-MFP in the Δ*yta10* yeast strain, Mdl2(1–5TM)[Mba1] and Mdl2(1–6TM)[Mba1] produced mostly *s*-Mgm1p in both the WT and Δ*yta10* yeast strains (Fig. 3C). The results of these control MFPs suggest that TM5 of Mdl2p is not membrane-inserted by the stop-transfer mechanism.

Next, Mdl2-MFP constructs were expressed in the *pam16-3* mutant strain to investigate the role of the PAM complex in the biogenesis of Mdl2p. Expression levels of Mdl2 (1–3TM), Mdl2 (1–4TM), Mdl2 (1–5TM) and Mdl2 (1–6TM) were very low in the *pam16-3* mutant strain (Fig. 3D). We questioned whether the membrane insertion of TM3–6 of Mdl2p is dependent on the PAM complex and whether inefficiently imported Mdl2p undergoes rapid degradation. Thus, Mdl2-MFP constructs were radiolabeled with [S^{35}]-Met for 5 min and were chased for the indicated times (Fig. 3E). L-MFPs appeared as the major products in *pam16-3* at the 0-min chase; however, *s*-Mgm1p appeared for Mdl2 (1–2TM) during the chase period and eventually reached ~50% at the 20-min time point, indicating that the insertion of the TM2 segment into the membrane is delayed. This delay may indicate that the stop-transfer membrane insertion of TM1 is followed by the TM2 membrane insertion from the IMS. L-MFP disappeared almost entirely in the 20-min chase for Mdl2 (1–3TM), Mdl2 (1–4TM), Mdl2 (1–5TM) and Mdl2 (1–6TM), suggesting that improperly sorted MFPs in the PAM-defective strain undergo degradation (Fig. 3E).

3.6. Different sorting mode of TM3 in Mdl1p and Mdl2p

Mdl1p and Mdl2p display high sequence homology, and the number, position and hydrophobicity of each protein's TM domains are also very similar (Fig. 4A) (Table 1). However, our results indicate that the mode of membrane insertion for TM3 of Mdl1p and Mdl2p differs; TM3 of Mdl2p is inserted into the inner membrane by the stop-transfer mechanism, whereas that of Mdl1p is not anchored via the same mechanism. To assess the formation of L-MFP and *s*-Mgm1p in more detail, first, we carried out pulse-chase experiments with the Mdl1 (1–3TM) and Mdl2 (1–3TM) constructs (Fig. 4B). For Mdl1 (1–3TM), three separate populations were detected at the 0-min chase time, with sizes corresponding to the precursor, L-MFP and *s*-Mgm1p. At longer chase time points, the precursor and L-MFP were no longer detected. Although we cannot rule out the possibility that the precursor and L-MFP were selectively degraded, these results may reflect a slow conversion of the precursor and L-MFP to *s*-Mgm1p. For Mdl2 (1–3TM), L-MFP was the major product at all chase times, indicating the membrane insertion of Mdl2 (1–3TM) (Fig. 4B).

Next, we swapped the TM3 of Mdl1(1–3TM) and Mdl2 (1–3TM) with or without the upstream loop domain (LD) (Fig. 4A). We included the LD because the membrane insertion of a TM domain can be influenced by the flanking loop [37]. Regardless of the presence of the loop domain from Mdl1p or Mdl2p, chimera proteins containing TM3 of Mdl2p predominantly produced L-MFP in the Δ*yta10* yeast strain (Fig. 4C). In contrast, chimera proteins containing TM3 of Mdl1p primarily generated *s*-Mgm1p (Fig. 4C). These results suggest that TM3 of Mdl2p contains a stop-transfer signal, whereas TM3 of Mdl1p does not. To confirm this result, constructs carrying only TM3 of Mdl1p or Mdl2p were prepared, and their

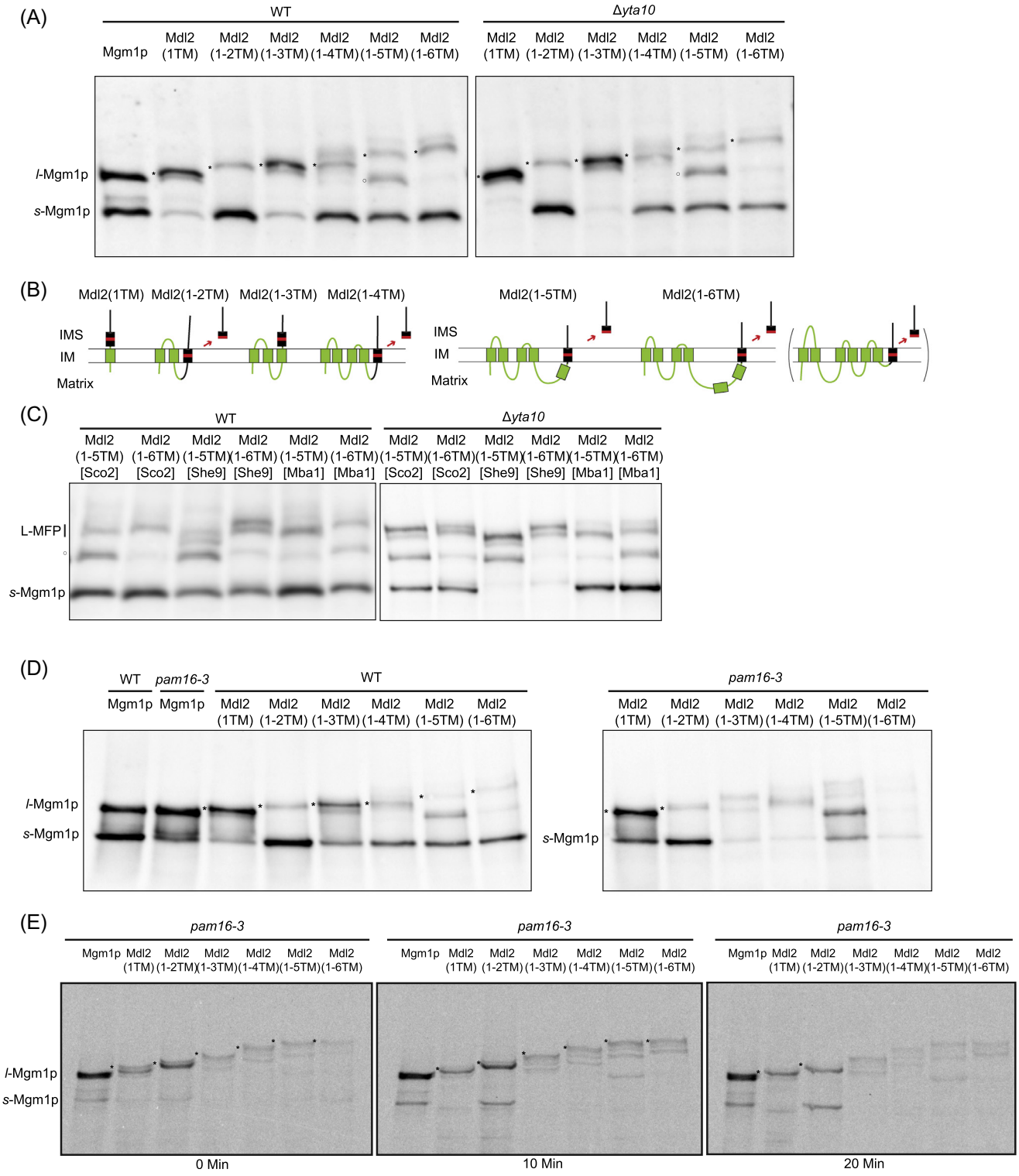

Fig. 3. Membrane insertion of Mdl2p, a homolog of Mdl1p. Yeast transformants of W303-1a and Δ*yta10* (A and C) and the *pam16-3* mutant or its isogenic WT strain (D) carrying different Mdl2-MFP constructs were grown in -Leu medium overnight at 30 °C. Samples were prepared and analyzed as in Fig. 2. (B) Scheme representing possible sorting mechanisms of Mdl2-MFPs. Domains of Mdl2p are shown in green. (E) The temperature-sensitive *pam16-3* mutant strain carrying the annotated Mdl2-MFP or Mgm1p were grown overnight at 24 °C and radiolabeled with [S^{35}]-Met for 5 min and chased for the indicated time points at a non-permissive temperature. Samples were immunoprecipitated with an anti-HA antibody and analyzed by SDS–PAGE and autoradiography. L-MFP is indicated with *asterisks*. Open circles represent unknown fragments. *l*-Mgm1p, long Mgm1 isoform; *s*-Mgm1p, short soluble Mgm1 isoform; L-MFP, long Mgm1 fusion protein.

membrane insertion efficiencies were assessed (Fig. 4D). Mdl1(3TM) predominantly generated *s*-Mgm1p, whereas Mdl2 (3TM) primarily produced L-MFP in Δ*yta10* strain, confirming that TM3 of Mdl2p contains a stop-transfer signal (Fig. 4D).

Upon examination of the Mdl1p and Mdl2p TM3 sequences (Fig. 4A), we observed five positions in which the Mdl1p residues had different physicochemical properties from Mdl2p. First, we noticed that a positively charged K is present at the C-terminal

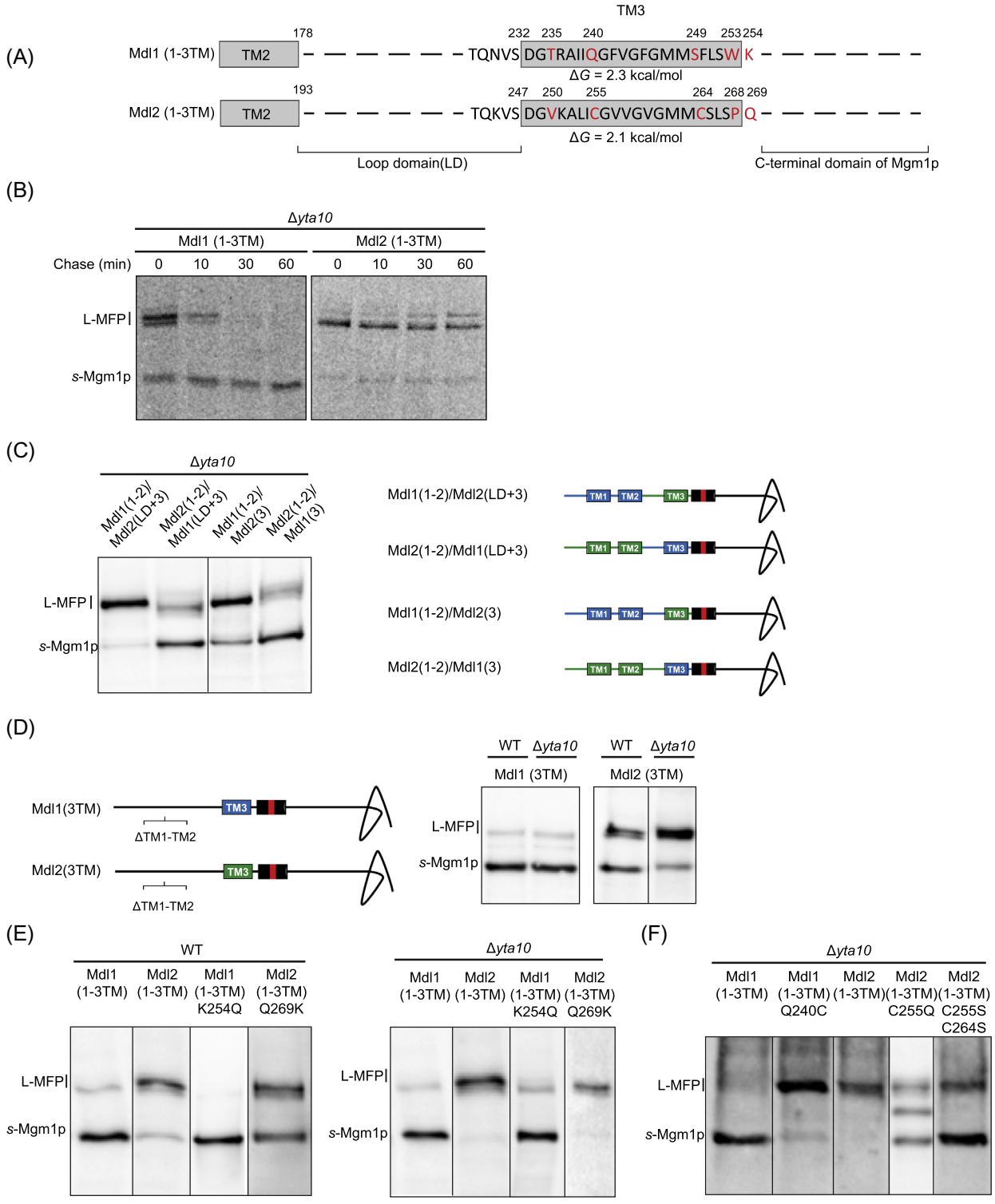

Fig. 4. Different membrane insertion modes for TM3 from Mdl1p and Mdl2p. (A) Sequence of TM3 and its flanking residues in Mdl1p and Mdl2p is shown. Both loop domains are 55 amino acids long (178–232 residues in Mdl1p, and 193–247 residues in Mdl2p). T235, Q240, S249, W253 and K254 in Mdl1p and V250, C255, C264, P268 and Q269 in Mdl2p were chosen for the residue-swapping experiments (red). TM domains are shown in the gray box. (B) Δ*yta10* cells carrying a plasmid encoding either Mdl1 (1–3TM) or Mdl2 (1–3TM) were grown at 30 °C and radiolabeled with [S^{35}]-Met for 5 min and chased for the indicated time points at 30 °C. Then, the samples were analyzed as in Fig. 3E. (C)–(F) Various Mdl1-MFPs or Mdl2-MFPs were transformed to the WT and Δ*yta10* yeast strains. Protein samples were prepared and analyzed as in Fig. 2.

end of TM3 in Mdl1, whereas Q is present in the analogous position in Mdl2p. To determine whether the presence of K promotes the import of Mdl1p TM3, we exchanged the residues at this position. The sorting pattern of TM3 of Mdl1(1–3TM)K254Q was not changed compared to Mdl1(1–3TM), indicating that the downstream residue does not affect the sorting of Mdl1p TM3 (Fig. 4E).

Although Mdl2(1–3TM)Q269 K generated ~50% *s*-Mgm1p compared to Mdl2 (1–3TM) in the WT strain, ~90% L-MFP was

observed in the Δ*yta10* yeast strain, indicating that most *s*-Mgm1p in the WT strain resulted from *m*-AAA protease action and that TM3 was sorted by the stop-transfer mode at the level of TIM23 (Fig. 4E). This result demonstrates that this residue does not affect the sorting of TM3 of Mdl1p or Mdl2p.

The other four TM3 residues with different physicochemical properties were individually swapped between Mdl1p and Mdl2p. Mdl1p mutants, T235V and W253P, and Mdl2p mutants, V250T and P269W, did not alter the sorting mode of Mdl1p or Mdl2p, indicating that these residues are not major determinants for TM3 sorting (data not shown). However, when Q240 was exchanged to C in Mdl1p, L-MFP was the major form in the Δ*yta10* yeast strain (Fig. 4F). This result indicates that the replacement of Q240 to C changed the mode of Mdl1p TM3 sorting to the stop-transfer mechanism. Similarly, when the corresponding TM3 residue position in Mdl2p, C255, was exchanged to Q, the level of L-MFP was significantly reduced in Δ*yta10* strain. When two C residues in the Mdl2p were changed to S, the level of L-MFP was dramatically reduced (Fig. 4F). These residue-swapping experiments suggest that Q in TM3 of Mdl1p and two Cs in TM3 of Mdl2p are critical determinants for import and membrane insertion by the TIM23 complex.

4. Discussion

The classic model of the TIM23-mediated sorting is that inner membrane proteins containing the N-terminal MTS are translated in the cytosol and are subsequently inserted into the mitochondrial inner membrane by the stop-transfer mechanism or the conservative sorting pathway. However, two independent studies demonstrate that more than one sorting mode can be used for membrane insertion of individual TM segments in multi-spanning inner membrane proteins [18,19].

In this study, we examined the mode of membrane insertion for individual TM segments of the multi-spanning inner membrane proteins, Mdl1p and Mdl2p *in vivo* by using the Mgm1 fusion protein approach. Although this approach has its limitations, we were able to demonstrate that the mode of membrane insertion for Mdl1p and Mdl2p differs despite the significant homology of these two proteins. For Mdl1p, TMs 1–2 are inserted into the membrane by the TIM23 complex from the IMS, and TM3 and TM5 are not laterally inserted by the TIM23 complex in the absence of downstream TM segments. For Mdl2p, TMs 1–4, but not TM5, are inserted into the inner membrane from the IMS. The results are summarized in Table 2.

Interestingly, although the hydrophobicity of the Mdl1p and Mdl2p TM3 segments are similar, the membrane insertion mode is different. We found that the sequence context within the TM segment is critical for the membrane insertion of the Mdl1p and Mdl2p TM segments by the TIM23 complex. In particular, two C residues in TM3 of Mdl2p and one Q residue in TM3 of Mdl1p are crucial for determining the sorting mode of Mdl1p and Mdl2p. When Q was introduced into the hydrophobic stretch of the cytochrome b2 (Cyb2)-CoxIV fusion protein, it was abnormally sorted into the matrix [38], suggesting that this Q residue may be an important determinant that either prevents the stop-transfer mode of membrane insertion or promotes import at the TIM23 complex. Furthermore, the observation that the C residue is not interchangeable with S indicates that the specific sequence context is more important for determining the mode of membrane insertion than the hydrophobicity. It is also possible that interactions between neighboring TM segments affect the mode of membrane insertion for multi-spanning membrane proteins.

Table 2
Summary of the membrane insertion data for individual TM segments of Mdl1p and Mdl2p by the TIM23 complex.

	TM	Membrane insertion		TM	Membrane insertion
Mdl1p	1	Stop-transfer	Mdl2p	1	Stop-transfer
	2	Insertion from the IMS		2	Insertion from the IMS
	3	No stop-transfer		3	Stop-transfer
	4	No stop-transfer		4	Insertion from the IMS
	5	No stop-transfer		5	No stop-transfer
	6	No stop-transfer		6	No stop-transfer

Acknowledgments

The authors thank the lab members for suggestions and comments on the work. This work was supported by a Basic Research Grant (2012-0001935) and a Global Research Network Grant (C00048) from the National Research Foundation of Korea to H.K.

References

[1] Schmidt, O., Pfanner, N. and Meisinger, C. (2010) Mitochondrial protein import: from proteomics to functional mechanisms. Nat. Rev. Mol. Cell Biol. 11, 655–667.
[2] Glick, B.S., Brandt, A., Cunningham, K., Muller, S., Hallberg, R.L. and Schatz, G. (1992) Cytochromes c1 and b2 are sorted to the intermembrane space of yeast mitochondria by a stop-transfer mechanism. Cell 69, 809–822.
[3] Chacinska, A. et al. (2005) Mitochondrial presequence translocase: switching between TOM tethering and motor recruitment involves Tim21 and Tim17. Cell 120, 817–829.
[4] van der Laan, M., Hutu, D.P. and Rehling, P. (2010) On the mechanism of preprotein import by the mitochondrial presequence translocase. Biochim. Biophys. Acta 1803, 732–739.
[5] Herrmann, J.M., Neupert, W. and Stuart, R.A. (1997) Insertion into the mitochondrial inner membrane of a polytopic protein, the nuclear-encoded Oxa1p. EMBO J. 16, 2217–2226.
[6] Hell, K., Herrmann, J.M., Pratje, E., Neupert, W. and Stuart, R.A. (1998) Oxa1p, an essential component of the N-tail protein export machinery in mitochondria. Proc. Natl. Acad. Sci. USA 95, 2250–2255.
[7] Preuss, M., Leonhard, K., Hell, K., Stuart, R.A., Neupert, W. and Herrmann, J.M. (2001) Mba1, a novel component of the mitochondrial protein export machinery of the yeast *Saccharomyces cerevisiae*. J. Cell Biol. 153, 1085–1096.
[8] Wagener, N., Ackermann, M., Funes, S. and Neupert, W. (2011) A pathway of protein translocation in mitochondria mediated by the AAA-ATPase Bcs1. Mol. Cell 44, 191–202.
[9] Meier, S., Neupert, W. and Herrmann, J.M. (2005) Proline residues of transmembrane domains determine the sorting of inner membrane proteins in mitochondria. J. Cell Biol. 170, 881–888.
[10] Neupert, W. and Herrmann, J.M. (2007) Translocation of proteins into mitochondria. Annu. Rev. Biochem. 76, 723–749.
[11] Herrmann, J.M. and Neupert, W. (2003) Protein insertion into the inner membrane of mitochondria. IUBMB Life 55, 219–225.
[12] Chacinska, A., Koehler, C.M., Milenkovic, D., Lithgow, T. and Pfanner, N. (2009) Importing mitochondrial proteins: machineries and mechanisms. Cell 138, 628–644.
[13] Koehler, C.M. et al. (1998) Tim9p, an essential partner subunit of Tim10p for the import of mitochondrial carrier proteins. EMBO J. 17, 6477–6486.
[14] Sirrenberg, C., Bauer, M.F., Guiard, B., Neupert, W. and Brunner, M. (1996) Import of carrier proteins into the mitochondrial inner membrane mediated by Tim22. Nature 384, 582–585.
[15] Sirrenberg, C., Endres, M., Folsch, H., Stuart, R.A., Neupert, W. and Brunner, M. (1998) Carrier protein import into mitochondria mediated by the intermembrane proteins Tim10/Mrs11 and Tim12/Mrs5. Nature 391, 912–915.
[16] Stein, I., Peleg, Y., Even-Ram, S. and Pines, O. (1994) The single translation product of the FUM1 gene (fumarase) is processed in mitochondria before being distributed between the cytosol and mitochondria in *Saccharomyces cerevisiae*. Mol. Cell. Biol. 14, 4770–4778.
[17] Ahmed, A.U. and Fisher, P.R. (2009) Import of nuclear-encoded mitochondrial proteins: a cotranslational perspective. Int. Rev. Cell. Mol. Biol. 273, 49–68.
[18] Park, K., Botelho, S.C., Hong, J., Osterberg, M. and Kim, H. (2013) Dissecting stop transfer versus conservative sorting pathways for mitochondrial inner membrane proteins in vivo. J. Biol. Chem. 288, 1521–1532.
[19] Bohnert, M., Rehling, P., Guiard, B., Herrmann, J.M., Pfanner, N. and van der Laan, M. (2010) Cooperation of stop-transfer and conservative sorting mechanisms in mitochondrial protein transport. Curr. Biol. 20, 1227–1232.
[20] Altschul, S.F., Madden, T.L., Schaffer, A.A., Zhang, J., Zhang, Z., Miller, W. and Lipman, D.J. (1997) Gapped BLAST and PSI-BLAST: a new generation of protein database search programs. Nucleic Acids Res. 25, 3389–3402.
[21] Altschul, S.F., Wootton, J.C., Gertz, E.M., Agarwala, R., Morgulis, A., Schaffer, A.A. and Yu, Y.K. (2005) Protein database searches using compositionally adjusted substitution matrices. FEBS J. 272, 5101–5109.

[22] Dean, M., Allikmets, R., Gerrard, B., Stewart, C., Kistler, A., Shafer, B., Michaelis, S. and Strathern, J. (1994) Mapping and sequencing of two yeast genes belonging to the ATP-binding cassette superfamily. Yeast 10, 377–383.
[23] Spee, J.H., de Vos, W.M. and Kuipers, O.P. (1993) Efficient random mutagenesis method with adjustable mutation frequency by use of PCR and dITP. Nucleic Acids Res. 21, 777–778.
[24] Oldenburg, K.R., Vo, K.T., Michaelis, S. and Paddon, C. (1997) Recombination-mediated PCR-directed plasmid construction in vivo in yeast. Nucleic Acids Res. 25, 451–452.
[25] Botelho, S.C., Osterberg, M., Reichert, A.S., Yamano, K., Bjorkholm, P., Endo, T., von Heijne, G. and Kim, H. (2011) TIM23-mediated insertion of transmembrane alpha-helices into the mitochondrial inner membrane. EMBO J. 30, 1003–1011.
[26] Heude, M., Fukuhara, H. and Moustacchi, E. (1979) Spontaneous and induced rho mutants of *Saccharomyces cerevisiae*: patterns of loss of mitochondrial genetic markers. J. Bacteriol. 139, 460–467.
[27] Tatsuta, T., Augustin, S., Nolden, M., Friedrichs, B. and Langer, T. (2007) M-AAA protease-driven membrane dislocation allows intramembrane cleavage by rhomboid in mitochondria. EMBO J. 26, 325–335.
[28] Frazier, A.E. et al. (2004) Pam16 has an essential role in the mitochondrial protein import motor. Nat. Struct. Mol. Biol. 11, 226–233.
[29] Arnold, I., Folsch, H., Neupert, W. and Stuart, R.A. (1998) Two distinct and independent mitochondrial targeting signals function in the sorting of an inner membrane protein, cytochrome c1. J. Biol. Chem. 273, 1469–1476.
[30] Young, L., Leonhard, K., Tatsuta, T., Trowsdale, J. and Langer, T. (2001) Role of the ABC transporter Mdl1 in peptide export from mitochondria. Science 291, 2135–2138.
[31] Gompf, S., Zutz, A., Hofacker, M., Haase, W., van der Does, C. and Tampe, R. (2007) Switching of the homooligomeric ATP-binding cassette transport complex MDL1 from post-translational mitochondrial import to endoplasmic reticulum insertion. FEBS J. 274, 5298–5310.
[32] Botelho, S.C., Tatsuta, T., von Heijne, G. and Kim, H. (2013) Dislocation by the m-AAA protease increases the threshold hydrophobicity for retention of transmembrane helices in the inner membrane of yeast mitochondria. J. Biol. Chem. 288, 4792–4798.
[33] Messerschmitt, M., Jakobs, S., Vogel, F., Fritz, S., Dimmer, K.S., Neupert, W. and Westermann, B. (2003) The inner membrane protein Mdm33 controls mitochondrial morphology in yeast. J. Cell Biol. 160, 553–564.
[34] Lode, A., Paret, C. and Rodel, G. (2002) Molecular characterization of *Saccharomyces cerevisiae* Sco2p reveals a high degree of redundancy with Sco1p. Yeast 19, 909–922.
[35] Schneider, H.C., Berthold, J., Bauer, M.F., Dietmeier, K., Guiard, B., Brunner, M. and Neupert, W. (1994) Mitochondrial Hsp70/MIM44 complex facilitates protein import. Nature 371, 768–774.
[36] van der Laan, M. et al. (2005) Pam17 is required for architecture and translocation activity of the mitochondrial protein import motor. Mol. Cell. Biol. 25, 7449–7458.
[37] Osterberg, M., Calado Botelho, S., von Heijne, G. and Kim, H. (2011) Charged flanking residues control the efficiency of membrane insertion of the first transmembrane segment in yeast mitochondrial Mgm1p. FEBS Lett. 585, 1238–1242.
[38] Beasley, E.M., Muller, S. and Schatz, G. (1993) The signal that sorts yeast cytochrome b2 to the mitochondrial intermembrane space contains three distinct functional regions. EMBO J. 12, 2303–2311.
[39] Bernsel, A., Viklund, H., Hennerdal, A. and Elofsson, A. (2009) TOPCONS: consensus prediction of membrane protein topology. Nucleic Acids Res. 37, W465–W468.
[40] Hessa, T. et al. (2007) Molecular code for transmembrane-helix recognition by the Sec61 translocon. Nature 450, 1026–1030.